one-electron energy change of the screened valence electrons $(\Delta H_{eff})_o$, the very large positive value of ΔL_o (for positive ΔE) is largely compensated by the negative value of ΔT_o and ΔC_{oc}. This results in a value of $(\Delta H_{eff})_o$ that is of the same order of magnitude as ΔC_o. Depending on the case, one of these two energy terms will make the most important contribution to ΔE.[7,17] Sometimes, but not always,[7] it will be ΔC_o.

Whether these conclusions can be maintained beyond the Hartree–Fock level, and whether they are valid for the exact (experimental) situation, is a question that can find only a partial answer. Indeed, for the exact wave functions, the distinction between open and closed shells becomes meaningless. But the question can be discussed for the global components ΔL, ΔT, and ΔC, which—in Hartree–Fock theory—are given by

$$\Delta L = \Delta L_c + \Delta L_o \qquad \Delta T = \Delta T_c$$
$$\Delta C = \Delta C + \Delta C_o + \Delta C_{oc} \tag{11}$$

The analysis of the experimental data presented in this paper shows that the energy sequence of the multiplets within a $3d^q$ configuration is determined by the electron–nuclear attraction L, *not* by the interelectronic repulsion C. The number of systems and states considered here is far from complete, but the present results suggest that Hartree–Fock theory is probably a reliable guide in providing a qualitatively correct picture of the excitation process.[17] Therefore, we have confidence in the Hartree–Fock predictions also for those cases where an exact analysis has not been carried out so far: examples are $4d^q$ and $5d^q$ systems,[7] f^n systems,[22] and especially molecular transition-metal complexes.[23–25]

Both conventional multiplet theory and ligand field theory are basically first-order perturbation approaches. The analysis of Table II shows that the conceptual framework underlying these classical theories is inadequate. Both theories are qualitatively very satisfactory, and they have an undeniable predictive value. But they fail (even qualitatively) in providing *the reason* that a certain energy pattern of the excited states is observed. The conventional textbook rationalization of multiplet theory, Hund's rules, and ligand field theory is basically too simplistic. One of the consequences is that phenomena such as high-spin/low-spin transitions, spin-pairing energy, the nephelauxetic effect, ligand field excitations, etc. should be reconsidered against the proper physical background.

(22) Vanquickenborne, L. G.; Pierloot, K.; Görller-Walrand, C. *Inorg. Chim. Acta* in press.
(23) Wachters, A. H. J.; Nieuwpoort, W. C. *Phys. Rev. B: Solid State* **1972**, *5*, 4291.
(24) Vanquickenborne, L. G.; Haspeslagh, L.; Hendrickx, M. In *The Chemistry of Excited States and Reactive Intermediates*; Lever, A. B. P., Ed.; ACS Symposium Series 307; Americian Chemical Society: Washington, DC, 1986; Chapter 2.
(25) Vanquickenborne, L. G.; Hyla-Kryspin, I.; Hendrickx, M. *Quantum Chemistry: The Challenge of Transition Metals and Coordination Chemistry*; Veillard, A., Ed.; Reidel: Dordrecht, The Netherlands, 1986; pp 225–234.

Contribution from the Chemistry Department, University of San Francisco, Ignatian Heights, San Francisco, California 94117-1080

Evidence for Specific Solvent–Solute Interactions as a Major Contributor to the Franck–Condon Energy in Intervalence-Transfer Absorptions of Ruthenium Ammine Complexes

Junghae P. Chang, Ella Y. Fung, and Jeff C. Curtis*

Received May 20, 1986

The relationship between the electrochemically determined redox asymmetry, $\Delta E_{1/2}$, and the spectroscopic intervalence-transfer band energy, E_{IT}, over a series of asymmetric dimers of the formulation $(bpy)_2Ru^{II}(Cl)pyzRu^{III}(NH_3)_4L^{4+}$ has been investigated in two ways. In the first method the unique ligand L is varied synthetically so as to manipulate the potential of the ruthenium–ammine end of the dimer. In the second method the solvent is varied so as to manipulate the potential of the ruthenium–ammine end via the well-known solvent donor number effect. Comparison of these two approaches reveals that there is a solvent donor number dependent contribution to the Frank–Condon barrier of approximately 0.006 eV/DN that completely overwhelms the dielectric continuum theory derived $(1/n^2 - 1/D_s)$ solvent dependence typically observed in symmetrical dimers. Implications with respect to the potential energy surfaces governing electron transfer in these systems are discussed.

Introduction

Considerable progress has been made in recent years in both understanding and experimentally elucidating the role of the solvent in optical and thermal electron-transfer processes in fluid solution.[1–4] The roles of both solvent dielectric[1a,3–6] and solvent dynamical[1f–k,2] properties have received careful attention. One of the most notable convergences between theory and experiment has been in the application of the dielectric continuum theory of the solvent reorganizational barrier as developed by Marcus[5] and

(1) (a) Creutz, C. *Prog. Inorg. Chem.* **1983**, *30*, 1. (b) Sutin, N. *Acc. Chem. Res.* **1982**, *15*, 275. (c) Sutin, N. *Prog. Inorg. Chem.* **1983**, *30*, 441. (d) Newton, M. D.; Sutin, N. *Annu. Rev. Phys. Chem.* **1984**, *35*, 437. (e) German, E. D.; Kuzuetsov, A. M. *Electrochim. Acta* **1981**, *26*, 1595. (f) Kjaer, A. M.; Ulstrup, J. *Inorg. Chem.* **1986**, *25*, 644. (g) Calef, D. F.; Wolynes, P. G. *J. Phys. Chem.* **1983**, *87*, 3387. (h) Calef, D. F.; Wolynes, P. G. *J. Chem. Phys.* **1983**, *78*, 470. (i) Van Der Swan, G.; Hynes, J. T. *Chem. Phys.* **1984**, *90*, 21. (j) Van Der Swan, G.; Hynes, J. T. *J. Chem. Phys.* **1982**, *76*, 2993. (k) Van Der Swan, G.; Hynes, J. T. *J. Chem. Phys.* **1983**, *78*, 4174.
(2) (a) Huppert, D.; Kanety, H.; Kosower, E. M. *Faraday Discuss. Chem. Soc.* **1982**, *74*, 161. (b) Kosower, E. M.; Huppert, D. *Chem. Phys. Lett.* **1983**, *96*, 433. (c) Gennett, T.; Milner, D. F.; Weaver, M. J. *J. Phys. Chem.* **1985**, *89*, 2787. (d) Hupp, J. T.; Liu, H. Y.; Farmer, J. K.; Gennett, T.; Weaver, M. J. *J. Electroanal. Chem. Interfacial Electrochem.* **1984**, *168*, 313. (e) Schmidt, J. A.; Siemialczuk, A.; Weedon, A. C.; Bolton, J. R. *J. Am. Chem. Soc.* **1985**, *107*, 642. (f) Pasman, P.; Mes, G.; Koper, W. W.; Verhoeven, J. W. *J. Am. Chem. Soc.* **1985**, *107*, 5839. (g) Kakitani, T.; Mataga, N. *Chem. Phys.* **1985**, *93*, 381. (h) Kakitani, T.; Mataga, N. *J. Phys. Chem.* **1985**, *89*, 4752. (i) Kakitani, T.; Mataga, N. *Ibid.* **1985**, *90*, 993.
(3) (a) Li, L. T.; Brubaker, C. H. *J. Organomet. Chem.* **1981**, *216*, 223. (b) Li, T. T.; Weaver, M. J.; Brubaker, C. H. *J. Am. Chem. Soc.* **1982**, *104*, 2381. (c) Chan, M.; Wahl, A. C. *J. Phys. Chem.* **1982**, *86*, 126. (d) Grampp, G.; Jaenicke, W. *J. Chem. Soc., Faraday Trans. 2* **1985**, *81*, 1035. (e) Grampp, G.; Jaenicke, W. *Chem. Phys. Lett.* **1984**, *112*, 263. (f) Grampp, G.; Jaenicke, W. *Ber. Bunsen-Ges. Phys. Chem.* **1984**, *88*, 325. (g) Russell, C.; Jaenicke, W. *J. Electroanal. Chem. Interfacial Electrochem.* **1984**, *180*, 205.
(4) (a) Meyer, T. J. *Acc. Chem. Res.* **1978**, *4*, 94. (b) Sullivan, B. P.; Curtis, J. C.; Kober, E. M.; Meyer, T. J. *Nouv. J. Chim.* **1980**, *4*, 643. (c) Powers, M. J.; Salmon, D. J.; Callahan, R. W.; Meyer, T. J. *J. Am. Chem. Soc.* **1976**, *98*, 6731. (d) Powers, M. J.; Meyer, T. J. *Inorg. Chem.* **1978**, *17*, 1785. (e) Powers, M. J.; Meyer, T. J. *J. Am. Chem. Soc.* **1978**, *100*, 4393. (f) Powers, M. J.; Meyer, T. J. *J. Am. Chem. Soc.* **1980**, *102*, 1289. (g) Powers, M. J.; Callahan, R. W.; Salmon, D. J.; Meyer, T. J. *Inorg. Chem.* **1976**, *15*, 1457. (h) Sullivan, B. P.; Meyer, T. J. *Inorg. Chem.* **1980**, *19*, 752.
(5) (a) Marcus, R. A. *J. Chem. Phys.* **1956**, *24*, 906. (b) Marcus, R. A. *Annu. Rev. Phys. Chem.* **1964**, *15*, 155.
(6) (a) Hush, N. S. *J. Chem. Phys.* **1958**, *28*, 962. (b) Hush, N. S. *Trans. Faraday Soc.* **1961**, *57*, 557. (c) Hush, N. S. *Prog. Inorg. Chem.* **1967**, *8*, 391.

0020-1669/86/1325-4233$01.50/0

Hush[6] to the kinetics of certain thermal electron-transfer reactions[3] and to the energies of the optical electron-transfer or intervalence-transfer (IT) absorption processes in mixed-valence, binuclear transition-metal complexes.[1a,4]

Spectroscopic studies of solvent effects on optical electron transfers are especially advantageous due to their relatively high experimental precision and convenience of execution. The energy of the IT transition in symmetric molecules such as in eq 1 is

$$(bpy)_2ClRu^{II}\text{–}L_b\text{–}Ru^{III}Cl(bpy)_2^{3+} \xrightarrow[E_{IT}]{h\nu} (bpy)_2ClRu^{III}\text{–}L_b\text{–}Ru^{II}Cl(bpy)_2^{3+*} \quad (1)$$

$$E_{IT} = X_{inner} + X_{outer} = E_{FC} \quad (2)$$

$$X_{outer} = e_0^2\left(\frac{1}{2a_1} + \frac{1}{2a_2} - \frac{1}{d}\right)\left(\frac{1}{n^2} - \frac{1}{D_s}\right) \quad (3)$$

determined primarily by the combined degrees of nuclear reorganization that occur within the inner coordination sphere of primary ligands and the outer, or solvation, sphere of solvent molecules around the complex when the electron is transferred.[7] Thus, the energy of the intervalence transfer is essentially a Franck–Condon energy in such cases. IT band energies have been demonstrated to vary in good agreement with the dielectric continuum theory (DCT) prediction as expressed in eq 3, both with respect to the distance between the sites d as the bridging ligand L_b is varied and with respect to the solvent dielectric function $(1/n^2 - 1/D_s)$, where e_0 is the electron charge, a_1 is the radius of the donor site, a_2 is the radius of the acceptor site, n is the refractive index, n^2 is the solvent's dielectric constant at optical frequencies, and D_s is the solvent's static dielectric constant (bpy = 2,2′-bipyridine).[1a,4]

The success of eq 3 has also been extended to metal-to-ligand charge-transfer (MLCT) transitions as in the complex $(bpy)_2Os^{II}Cl(N\text{-Methyl-4,4′-bipyridinium})^{3+}$.[8]

The situation is more complicated, however, if there exists the possibility for strong, specific solvent–solute interactions as has been demonstrated, for example, to be the case in a study of the solvatochromism of the MLCT and LMCT transitions in ruthenium(II) and -(III) ammine complexes.[9] In these complexes it was shown that the solvatochromism of the charge-transfer transitions was due primarily to the strong solvent dependence of the $Ru^{II/III}$–ammine redox potential and the resulting variations in the ground- and excited-state energy gap. The solvatochromism correlated well with the Lewis base strength of the solvent as measured by the Gutmann donor number (DN)[10] and by other known indicators of hydrogen bond *acceptance* ability.[11] It was also recognized that there might be a DN-dependent contribution to the outer-sphere reorganization energy X_{outer}.

A growing body of work in this regard on thermal electron transfers has shown both theoretical and experimental evidence for significant noncontinuum effects on the thermodynamics and kinetics of both heterogeneous (electrode) and homogeneous (bimolecular) electron-transfer reactions for ammine-ligand- and aquo-ligand-bearing transition-metal redox couples.[12–15]

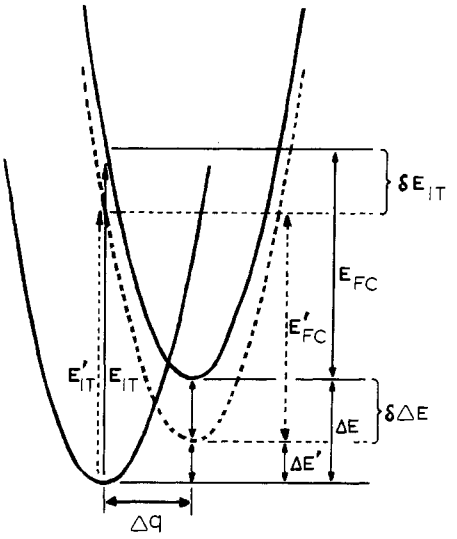

Figure 1. Schematic representation of the potential energy surfaces for a redox-asymmetric mixed-valence dimer where the asymmetry ΔE is manipulated without change in the Franck–Condon energy E_{FC}.

In this work we have undertaken to quantitatively assess the importance of these specific solvent–solute interactions as contributors to the Franck–Condon barrier to optical electron transfer in redox asymmetric mixed-valence systems such as shown in (4), where pyz = pyrazine and L is varied over a range of ligands (see Tables II and III).

$$(bpy)_2ClRu^{II}\text{–pyz–}Ru^{III}(NH_3)_4\text{–}L^{4+} \xrightarrow[E_{IT}]{h\nu} (bpy)_2ClRu^{III}\text{–pyz–}Ru^{II}(NH_3)_4\text{–}L^{4+*} \quad (4)$$

Figure 1 illutrates the relationship between the potential-energy surfaces for the ground- and excited-state redox isomers of an asymmetric system. ΔE represents the thermodynamic internal energy difference between the two thermally equilibrated redox isomers, E_{IT} represents the energy of the vertical spectroscopic transition from the lower to the upper surface, and Δq represents the total amount of nuclear reorganization in both the inner and the outer spheres that takes place upon thermal electron transfer. The nuclear coordinate Δq represents a one-dimensional projection of all the nuclear displacements, both reactant and solvent, that occur upon electron transfer. Equation 2 must now be modified to include the ΔE term:

$$E_{IT} = E_{FC} + \Delta E \quad (5)$$

In the simplest case, a variation in the redox asymmetry $\delta(\Delta E)$ will show up spectroscopically as an equivalent variation in the energy of the intervalence-transfer band δE_{IT}. If, however, as ΔE is varied there are any simultaneous changes in Δq or in one of the many force constants defining the shape of the upper surface, then the quantity $\delta E_{IT}/\delta(\Delta E)$ will deviate from unity.

The key to the work reported on here lies in the fact that it is possible to vary ΔE and hence monitor $\delta E_{IT}/\delta(\Delta E)$ in systems as shown in eq 4 by *two* different methods. One method is to "tune" ΔE via *synthetic* variations in L so as to selectively vary the redox potential of the ammine-bearing end of the dimer.[16,17]

(7) Due to the nondegenerate nature of the Ru^{II} t_{2g} orbital set and the existence of excited spin–orbit states on the spectroscopically produced Ru^{III} site, it has been concluded that the measured λ_{max} for an intervalence transition such as that shown in eq 1 is actually the result of a superposition of at least three bands and is probably shifted about 1500 cm^{-1} (0.186 eV) to the blue from the lowest energy component. See: Kober, E. M.; Goldsby, K. A.; Narayana, D. N. S.; Meyer, T. S. *J. Am. Chem. Soc.* **1983**, *105*, 4303.

(8) Kober, E. M. Ph.D. Dissertation, The University of North Carolina at Chapel Hill, 1981.

(9) Curtis, J. C.; Sullivan, B. P.; Meyer, T. J. *Inorg. Chem.* **1983**, *22*, 224.

(10) Gutmann, V. *The Donor-Acceptor Approach to Molecular Interactions*; Plenum: New York, 1978.

(11) (a) Marcus, Y. *J. Solution Chem.* **1984**, *13*, 599. (b) Kamlet, M. J.; Taft, R. W. *J. Am. Chem. Soc.* **1976**, *98*, 377. (c) Arnett, E. M.; Mitchell, E. J.; Murty, T. S. S. R. *J. Am. Chem. Soc.* **1974**, *96*, 3875.

(12) (a) Sahami, S.; Weaver, M. J. *J. Electroanal. Chem. Interfacial Electrochem.* *122*, 171. (b) Hupp, J. T.; Weaver, M. J. *J. Phys. Chem.* **1984**, *88*, 1860. (c) Hupp, J. T.; Weaver, M. J. *Inorg. Chem.* **1984**, *23*, 3639. (d) Hupp, J. T.; Weaver, M. J. *J. Phys. Chem.* **1985**, *89*, 1601.

(13) (a) Meyer, U.; Kotocova, A.; Gutmann, V.; Gergev, W. *J. Electroanal. Chem.* **1977**, *100*, 875. (b) Gritzner, G.; Danksagmuller, K.; Gutmann, V. *Ibid.* **1979**, *72*, 177. (c) Kotocova, A.; Meyer, U. *Collect. Czech. Chem. Commun.* **1980**, *45*, 335. (d) Meyer, U.; Gergev, W.; Gutmann, V.; Rechberger, P. *Z. Anorg. Allg. Chem.* **1980**, *464*, 200. (e) Gutmann, V. *Electrochim. Acta* **1978**, *21*, 661.

(14) (a) Tweedle, M. F.; Wilson, L. J. *J. Am. Chem. Soc.* **1976**, *98*, 4824. (b) Kadish, K. N.; Das, K.; Schaeper, D.; Merrill, C. L.; Welch, B. R.; Wilson, L. J. *Inorg. Chem.* **1980**, *19*, 2816. (c) Zhu, T.; Su, C. H.; Schaeper, D.; Lemke, B. K.; Wilson, L. J.; Kadish, K. M. *Inorg. Chem.* **1984**, *23*, 4345.

(15) Lay, P. A. *J. Phys. Chem.* **1986**, *90*, 878.

(16) (a) Malouf, G.; Ford, P. C. *J. Am. Chem. Soc.* **1977**, *99*, 7213. (b) Ford, P. C. *Rev. Chem. Intermed.* **1979**, *2*, 267.

The second approach is to vary the *solvent* and thus selectively affect the potential of the ammine-bearing end via the well-known solvent donor number dependency of the redox potentials of such groups.[9,12a,b,13,14b] Any systematic differences observed in the $\delta E_{IT}/\delta(\Delta E)$ values obtained by these two approaches should be informative with regard to possible variations in the Franck–Condon barrier E_{FC} as ΔE is manipulated.

As will be seen in the following development, these expectations are indeed borne out, and a strong donor number dependent contribution to E_{FC} is revealed.

Experimental Section

Synthesis. $(bpy)_2Ru^{II}Cl_2$ was synthesized according to the literature method.[18]

$(bpy)_2Ru^{II}Cl(pyz)PF_6$ monomer was synthesized according to a slight modification of the method due to Sullivan.[4h] A 0.5-g amount of $Ru(bpy)_2Cl_2$ was added to 60 mL of 1:1 ethanol/water and heated at reflux for 45 min in the presence of a 4-fold molar excess of pyrazine ligand (Aldrich). A 5-fold molar excess of NH_4PF_6 solid (Alfa) was added after the mixture was cooled, and the ethanol was removed by rotory evaporation with heating. The crude PF_6^- salt of the product was isolated by filtration and then reprecipitated once by dissolution in a minimum volume of acetone followed by filtration into 8 volumes of stirring anhydrous ether. The pure, red-black $(bpy)_2RuCl(pyz)PF_6$ was isolated chromatographically on alumina as the main red band using a 3:1 toluene/acetonitrile eluent containing 1% methanol. Typical yields were 80%. The redox potential of this molecule was found to be 0.838 V vs. SCE in good agreement with previous reports.[4c]

$(NH_3)_5Ru^{III}Cl(Cl)_2$. This starting material was synthesized from $Ru^{III}Cl_3{\cdot}nH_2O$ (Alfa) with use of the method of Clarke.[19] A 5.00-g amount of $Ru^{III}Cl_2{\cdot}nH_2O$ was stirred overnight with 62.6 mL of 64% hydrazine and 62.5 mL of H_2O to yield a purple-red solution. To this mixture, which was in an ice bath, was slowly added 125 mL of 12 M HCl, and the resulting mixture was then heated at reflux for 2 h. The yellow $(NH_3)_5RuCl_3$ product was isolated by filtration after it was chilled at 0 °C for at least 3 h. Typical yields were 80%. Trace NH_4Cl impurities could be removed by a single recrystallization from 0.1 M HCl.

$(NH_3)_5RuOH_2(PF_6)_2$. This reagent was synthesized according to the method reported in ref 9 and kept in a desiccator at 0 °C. It was found to retain its synthetic utility for several months upon careful storage.

***trans*-$SO_2Ru^{II}(NH_3)_4Cl_2$** was synthesized from the pentaammine trichloride with use of the methods outlined by Clarke[19] and Vogt[20] (see also ref 9).

***trans*-$LRu^{III}(NH_3)_4SO_4Cl$ (L = 3,5-Me_2-py, py, 4-Me-py, 4-Ac-py, 4-$CONH_2$-py (Isonicotinamide), 3-Cl-py, 3-F-py, 2,6-Me_2-pyz, bpy (–NH_3), phen (–NH_3)).** The *trans*-$LRu^{II}(NH_3)_4SO_2Cl_2$ intermediate was made by stirring 0.1–0.4 g of *trans*-$SO_2Ru^{II}(NH_3)_4Cl_2$ in the presence of excess L in 50–60 °C H_2O for 10–30 min. In the case of the more hydrophobic ligands such as 3,5-Me_2-py or phen, addition of 15% acetone and use of the longer reaction times were necessary to ensure complete reaction (reaction with the chelates bpy or phen also involves loss of one equatorial ammine group to yield a triammine product). *It was found to be important in this procedure that the ligand be added to the water first.* Heating of the *trans*-$SO_2Ru^{II}(NH_3)_4Cl_2$ starting material in water alone for any period of time resulted in impurities. After reaction the *trans*-$LRuSO_2(NH_3)_4Cl_2$ product could be isolated in quantitative yield by addition of 10 volumes of reagent grade acetone. These products were typically light orange to pinkish red. The product was then dissolved in a minimum of H_2O and oxidized to *trans*-$LRu^{III}(NH_3)_4SO_4Cl$ by slow addition of 1:1 30% H_2O_2/0.2 M HCl. Complete reaction was signalled by a color change to light yellow or orange after 2–10 min. The product was precipitated by addition of 10 volumes of reagent acetone. Yields ranged from 60 to 90%. These products were stable for months upon storage at 0 °C under desiccation.

***trans*-$LRu^{II}(NH_3)_4OH_2(PF_6)_2$.** These complexes were synthesized analogously to the pentaammine aquo complex.[9] In a typical preparation 0.10 g of *trans*-$pyRu^{III}(NH_3)_4SO_4Cl$ was reduced in 1–3 mL of H_2O over a Zn/Hg amalgam for 10 min. The resulting orange-red solution was transferred under argon to a flask containing a 10-fold molar excess of solid NH_4PF_6. This mixture was stirred under Ar for 5 min and then chilled in a refrigerator. The product (yellow for L = py, red for L = bpy) was isolated by filtration under Ar and washed with anhydrous ether. Yields varied according to L: e.g. 89% for L = 3-Cl-py, 35% for L = 4-Cl-py. These reagents maintained their synthetic utility for up to several months when stored at 0 °C under desiccation. In some cases a slight discoloration to green or brown was noted over time. These compounds still worked in subsequent dimer syntheses but tended to give lesser yields and poorer initial purities.

$(bpy)_2Ru^{II}Cl(pyz)Ru^{II}(NH_3)_4L(PF_6)_3$. Method A. In this approach a 3-fold molar excess of the *trans*-$LRu^{II}(NH_3)_4OH_2(PF_6)_2$ monomer is reacted with the $(bpy)_2Ru^{II}Cl(pyz)PF_6$ monomer (typically 0.1 g) in ~15 mL of Ar-degassed acetone at 40 °C for 8–24 h. The crude, dark purple dimer $(bpy)_2Ru^{II}Cl(pyz)Ru^{II}(NH_3)_4L^{3+}$ is isolated as a chloride salt from this mixture by addition of 3 mL of a saturated solution of tetraethylammonium chloride in 7:3 acetone/methanol. The chloride salt is isolated by filtration, washed with acetone, and dried. This is converted to the PF_6^- salt by dissolving the chloride in water, filtering the mixture, and then adding an excess of NH_4PF_6 and collecting the crude PF_6^- salt. In order to obtain informative electrochemical data as to the purity of the compound at this stage, it must be reisolated from acetone/ether.

Method B. In this mixed-solvent approach the aquo compound is not isolated itself but is generated as needed from the more stable SO_4 complex. A 3-fold molar excess (typically 0.15 g) of *trans*-$LRu^{III}(NH_3)_4SO_4Cl$ is reduced for 10 min over Zn/Hg in 2–3 mL of H_2O and then added to an Ar-degassed solution of $(bpy)_2RuCl(pyz)PF_6$ in 50:50 acetone/ethanol (2–3 mL). This ternary solvent mixture is heated at 40–50 °C for at least 12 h. During this time the reaction mixture slowly changes from red-brown to the purple color characteristic of the dimeric product. After the reaction is judged complete, a 6–8-fold molar excess of NH_4PF_6 and 8–10 mL of H_2O are added. The PF_6^- salt is precipitated by removing the volatile solvents slowly on a rotary evaporator. Care should be taken not to allow the flask to go to dryness, as this leads to the formation of rather bothersome mixed salts. The crude PF_6^- salt is then isolated by filtration and dried.

Purification. The crude dimers synthesized by these methods contain both unreacted $(bpy)_2RuCl(pz)^+$ monomer and $[LRu^{III}(NH_3)_4]_2O^{4+}$ oxo-bridged impurities. (The latter of these is evident in the electrochemistry in acetonitrile as a low-potential wave in the neighborhood of 0.2 V vs. SCE.) Both of these impurities can be removed by repeated interconversion between chloride and PF_6^- salts. The reddish $(bpy)_2RuCl(pyz)^+$ monomer remains partially soluble in the acetone filtrate after chloride precipitation of the dimer from acetone, and the oxo-bridged ammine dimer remains in the H_2O filtrate after PF_6^- precipitation of the dimer from water. In no cases were more than three interconversions required. Partial reprecipitation from chilled acetone (2 mL) by slow addition of Et_2O so as to isolate three fractions of solid was also a useful method.

Microanalytical data (Berkeley Chemical Analytical Services) for all the compounds analyzed are as follows. Anal. Calcd (found) for $(bpy)_2RuCl(pyz)Ru(NH_3)_5(PF_6)_3{\cdot}H_2O$: C, 24.66 (24.39); H, 3.19 (3.17); N, 13.24 (12.19); C/N, 1.86 (2.00). Calcd (found) for $(bpy)_2RuCl(pyz)Ru(NH_3)_4py(PF_6)_3{\cdot}2H_2O$: C, 27.89 (27.84); H, 3.31 (2.98); N, 12.39 (11.82); C/N, 2.25 (2.36). Calcd (found) for $(bpy)_2RuCl(pyz)Ru(NH_3)_3(bpy)(PF_6)_3{\cdot}3H_2O$: C, 30.77 (30.55); H, 3.27 (3.83); N, 11.66 (11.21); C/N, 2.64 (2.73). Calcd (found) for $(bpy)_2RuCl(pyz)Ru(NH_3)_4(3,5\text{-}Me_2\text{-}py)(PF_6)_3{\cdot}(CH_3)_2CO$: C, 31.44 (31.57); H, 3.65 (3.13); N, 11.91 (11.29); C/N, 2.264 (2.80). Calcd (found) for $(bpy)_2RuCl(pyz)Ru(NH_3)_4(4\text{-}Me\text{-}py)(PF_6)_3{\cdot}(CH_3)_2CO$: C, 30.84 (29.67); H, 3.53 (3.08); N, 12.04 (11.78); C/N, 2.56 (2.52).

$Fe^{III}(bpy)_3(PF_6)_3$ Oxidant. The $Fe^{II}(bpy)_3(PF_6)_2$ starting material was made by heating 1 g of $Fe(NH_4)_2(SO_4)_2{\cdot}6H_2O$ in a 4-fold molar excess of 2,2′-bipyridine in 100 mL of boiling water for 45 min to yield a bright red solution. Addition of 3 equiv of NH_3PF_6 precipitated the crude red solid $Fe^{II}(bpy)_2(PF_6)_2$. This material was dissolved in a minimum volume of acetone and filtered into ether for isolation and for removal of unreacted 2,2′-bpy. The Fe^{III} form was generated by dissolving 0.1–0.2 g of the Fe^{II} in 5 mL of acetonitrile acidified with 1–2 drops of concen-

(17) (a) Curtis, J. C.; Meyer, T. J. *Inorg. Chem.* **1982**, *21*, 1562. (b) Toma, H. *Can. J. Chem.* **1979**, *57*, 2079. (c) Toma, H. *J. Chem. Soc., Dalton Trans.* **1980**, *3*, 471.
(18) Sullivan, B. P.; Salmon, D. J.; Meyer, T. J. *Inorg. Chem.* **1978**, *17*, 3334.
(19) Clarke, R. E. Masters Thesis, University of California at Santa Barbara, 1978.
(20) Vogt, L. H.; Katz, J. S.; Wiberly, S. E. *Inorg. Chem.* **1965**, *4*, 1156.
(21) $\Delta E_{1/2}$ in the $[(bpy)_2RuCl]_2pyz(PF_6)_2$ dimer studied by Callahan et al.[22] is 0.12 V in acetonitrile. This splitting is due primarily to electrostatic and secondarily to delocalization stabilizations of the mixed-valence II,III redox state relative to the II,II and III,III states. For the deca-ammine pyrazine-bridged ion $[(NH_3)_5Ru]_2pyz(PF_6)_2$ in acetonitrile $\Delta E_{1/2}$ = 0.430 V[23] and the relative importances of the electrostatic and delocalization contributions are unclear. For the dimers studied in this work the former effect probably predominates and will likely be somewhat increased compared to that in the Callahan dimer due to the higher charge density at the ammine end.
(22) Callahan, R. W.; Keene, F. R.; Meyer, T. J.; Salmon, D. J. *J. Am. Chem. Soc.* **1977**, *99*, 1064.
(23) de la Rosa, R.; Chang, P. J.; Salaymeh, F.; Curtis, J. C. *Inorg. Chem.* **1985**, *24*, 4229.

Table I. Solvents Used in This Study and Their Donor Number, $1/n^2 - 1/D_s$, Acceptor Number, $1/D_s$, and E_{Fc/Fc^+} Values

no.	solvent	DN[a]	$1/n^2 - 1/D_s$[b]	AN[a]	D_s[b]	E_{Fc/Fc^+},[c] V
1	nitromethane (NM)	2.7	0.4978	20.5	38.57	0.309
2	nitrobenzene (NB)	4.4	0.3851	14.8	34.82	0.371
3	benzonitrile (BN)	11.3	0.3885	15.5	25.2	0.388
4	acetonitrile (AN)	14.1	0.5289	19.3	37.5	0.376
5	tetramethylene sulfone (TMS)	14.8				0.389
6	propylene carbonate (PC)	15.1	0.4811	18.3	(63)	0.359
7	butyronitrile (BT)	16.6	0.4816		20.3	0.384
8	acetone (AC)	17	0.4934	12.5	20.74	0.463
9	trimethyl phosphate (TMP)	23				0.464
10	dimethylformamide (DMF)	26.6	0.4637	16	36.7	0.460
11	dimethylacetamide (DMA)	27.8	0.4587	13.6	37.78	0.478
12	dimethyl sulfoxide (Me_2SO)	29.8	0.4372	19.3	48.9	0.433

[a] Taken from ref 5. [b] Taken from: Koppel, I. A.; Palm, V. A. In *Advances in Linear Free Energy Relationships*; Chapman, N. B., Shorter, J., Eds.; Plenum: London, 1972; pp 254–258. [c] Measured via differential pulse polarography at a Pt disk in 0.1 M TEAH (1 mV/s sweep rate, 5-mV pulse amplitude, 0.2-s drop time).

Table II. Spectroscopic and Electrochemical (vs. SCE) Data for the Molecules $(bpy)_2Ru^{II}Cl(pyz)Ru^{III}(NH_3)_4L^{4+}$ in Acetonitrile

no.	ligand	λ_{max}(IT), nm	ϵ_{max}, M^{-1} cm^{-1}	$\Delta\nu_{1/2}$, eV	E_{IT}, eV	$E_{1/2}(Ru_a)$, V	$E_{1/2}(Ru_b)$, V	$\Delta E_{1/2}$, V
1	NH_3	1035 ± 10	1300	0.678	1.198 ± 0.01	0.553 ± 0.003	0.973 ± 0.003	0.420 ± 0.005
2	4-Me-py	1180 ± 20	1240	0.673	1.051 ± 0.018	0.684	0.983	0.296
3	3,5-Me_2-py	1160	713	0.701	1.07	0.667	0.963	0.296
4	py	1176	1340	0.679	1.046	0.722	1.005	0.283
5	3-F-py	1266 ± 20	918	0.635	0.99	0.709	0.937	0.228
6	4-Ac-py	1190	518	0.674	1.04	0.762	0.990	0.228
7	3-Cl-py	1308 ± 20	1082	0.614	0.95	0.769	1.001	0.223
8	4-C(O)NH_2-py	1232	490	0.733	1.002	0.754	0.970	0.221
9	2,6-Me_2-pz	1304	868	0.665	0.950	0.812	0.987	0.175
10	bpy (-NH_3)	1313	400	0.70	0.954	0.815	0.975	0.160
11	phen (-NH_3)	1310	826	0.736	0.947	0.851	1.000	0.149

[a] Obtained by doubling the value from the low-energy side of the band. [b] Experimental uncertainty in λ_{max}(IT) is estimated at ±10 nm except where noted.

Table III. Spectroscopic and Electrochemical (vs. SCE) Data for the Molecules $(bpy)_2Ru^{II}Cl(pz)Ru^{III}(NH_3)_4L^{4+}$ in DMF

no.	ligand	λ_{max}(IT), nm	ϵ_{max}, M^{-1} cm^{-1}	$\Delta\nu_{1/2}$, eV	E_{IT}, eV	$\Delta E_{1/2}(Ru_a)$, V	$\Delta E_{1/2}(Ru_b)$, V	$\Delta E_{1/2}$, V
1	NH_3	822 ± 10	590	0.677	1.512 ± 0.018	0.255 ± 0.003	0.975 ± 0.003	0.720 ± 0.005
2	4-Me-py	912	510	0.636	1.360	0.424	0.972	0.548
3	3,5-Me_2-py	872 ± 15	403	0.720	1.348	0.450	0.983	0.531
4	py	900 ± 5	480	0.674	1.378	0.455	0.996	0.538
6	4-Ac-py	902	313	0.658	1.370	0.437	0.964	0.527
7	3-Cl-py	940	407	0.700	1.319	0.485	1.00	0.515
8	4-C(O)NH_2-py	905	235	0.663	1.364	0.505	0.982	0.477
9	2,6-Me_2-pz	920	315	0.680	1.356	0.484	0.974	0.490
10	bpy (-NH_3)	975	212	0.700	1.272	0.692	0.978	0.326
11	phen (-NH_3)	1015	230		1.222	0.628	0.973	0.345

trated HPF_6. A saturated solution of ceric ammonium nitrate in acetonitrile was then added dropwise until the solution turned from red to greenish blue. This solution was then filtered into stirring anhydrous ether to precipitate the light blue $Fe^{III}(bpy)_3(PF_6)_3$ solid. This oxidant could be used stoichiometrically to oxidize solutions of II,II dimers as long as it retained its blue color (up to 4 months if care was taken to store it in a desiccator). Exposure to moisture, however, resulted in a rapid return to the red Fe^{II} form and loss of oxidizing power.

Tetraethylammonium Hexafluorophosphate (TEAH). TEAH electrolyte was synthesized by heating 25 g of tetraethylammonium bromide (Aldrich) in rapidly stirring H_2O (250 mL) with a 20% molar excess of KPF_6 (Alfa). After 20 min at 70–80 °C and subsequent cooling the resulting crude TEAH solid was filtered off and washed with cold water. Trace bromide was removed by dissolving this solid in a minimum of acetone and filtering into a stirring, saturated H_2O/KPF_6 solution of at least 6-fold larger volume. The resulting precipitate was collected by filtration and dried in vacuo. Yields were typically 70–80%. Recrystallization from hot ethanol gave white crystals.

Electrochemical Measurements. The electrochemical measurements were made with use of an IBM 225EC electrochemical analyzer using an IBM cell that was sealed from the atmosphere after assembly. Measurements were performed on 1.5-mL solvent volumes with 0.1 M TEAH as supporting electrolyte and ~0.1 mM complex. Most of the solvents could be used as received after at least 8 h of standing over 3-Å molecular sieves. In cases where large background currents due to impurities or water were encountered, it was found that passing the solvent over a column of activated alumina prior to addition of TEAH led to some improvement (NM, BN, AN, DMA; see Table I for solvent abbreviations). In the very low donor number solvents such as NM or NB it was found that the redox potential of the ammine-bearing end of a given dimer (the more cathodic wave in all these systems) would drift slowly to lower values with time upon standing. This was probably due to preferential solvation of the ammine-bearing end of the molecule by trace water entering the system neither from the reference electrode or the air. This drift could be *reversed* back to the original value by addition of 6–10 3-Å molecular sieves and 3 min of standing. From this we conclude that our potential data are not unduly influenced by trace water as a contaminant.

The potential of Fc/Fc^+ in each solvent is listed in Table I. These potentials were obtained by using the differential pulse polarography technique at a freshly polished Pt-disk electrode. It was found that potentials measured by DPP were far less influenced by trace monomeric impurities, closely spaced waves, or slight background currents than potentials measured by cyclic voltammetry.

Spectrophotometric Measurements. Near-infrared spectra were recorded on a Perkin-Elmer 330 UV–vis–near-IR spectrophotometer with the slit under automatic servo control. Spectra were obtained by stepwise titration of the II,II dimer to maximum absorbance and then slightly past with use of the solid $Fe^{III}(bpy)_2(PF_6)_3$ as oxidant.

Results and Discussion

Electroanalytical and spectral data for the dimers are listed in Tables II–V. The substantial solvent effect on the electrochemistry of the L = py dimer is shown for acetonitrile and DMF

Table IV. Spectroscopic and Electrochemical (vs. Fc/Fc$^+$) Data for the Dimer $(bpy)_2Ru^{II}Cl(pyz)Ru^{III}(NH_3)_5^{4+}$ in Various Solvents

no.	solvent	λ_{max}(IT),[c] nm	ϵ_{max}, M^{-1} cm^{-1}	$\Delta\nu_{1/2}$,[a] eV	E_{IT}, eV	$E_{1/2}(Ru_a)$, V	$E_{1/2}(Ru_b)$, V	$\Delta E_{1/2}$, V	$E_{IT} - \Delta E_{1/2}$, eV
1	NM	1248 ± 15[b] 1332	1245	0.610	0.994 ± 0.010	0.641	0.315	0.315	0.079
2	NB	1210[b] 1315	1300	0.641	1.025	0.229	0.547	0.316	0.709
3	BN	1084[b] 1080	950	0.688	1.144	0.149	0.549	0.400	0.744
4	AN	1029[b] 1035	1300	0.678	1.205	0.174	0.592	0.418	0.787
5	TMS	980	1000	0.704	1.265	0.076	0.614	0.538	0.727
6	PC	963	740	0.636	1.290	0.061	0.596	0.535	0.755
7	BT	1046	850	0.680	1.186	0.152	0.552	0.400	0.786
8	AC	980[b] 975	1030	0.703	1.205	−0.041	0.506	0.547	0.718
9	TMP	872	690	0.649	1.422	−0.052	0.581	0.633	0.789
10	DMF	818[b] 822	590	0.677	1.516	−0.205	0.515	0.720	0.796
11	DMA	824	550	0.652	1.505	−0.198	0.516	0.714	0.791
12	Me_2SO	780	515	0.717	1.589	−0.197	0.548	0.745	0.844

[a] Via doubling of low-energy side. [b] In 0.1 M TEAH. [c] Experimental uncertainty in λ_{max}(IT) estimated at ±10 nm except where noted.

Table V. Spectroscopic and Electrochemical (vs. Fc/Fc$^+$) Data for the Dimer $(bpy)_2Ru^{II}Cl(pyz)Ru^{III}(NH_3)_4py^{4+}$ in Various Solvents

no.	solvent	λ_{max}(IT),[c] nm	ϵ_{max}, M^{-1} cm^{-1}	$\Delta\nu_{1/2}$,[a] eV	E_{IT}, eV	$E_{1/2}(Ru_a)$, V	$E_{1/2}(Ru_b)$, V	$\Delta E_{1/2}$, V	$E_{IT} - \Delta E_{1/2}$, eV
1	NM	1620 ± 15[b] 1600	1900	0.226	0.769 ± 0.010	0.471 ± 0.003	0.641 ± 0.003	0.170 ± 0.005	0.599 ± 0.015
2	NB	1608[b] 1610	1500	0.290	0.771	0.369	0.565	0.196	0.575
3	BN	1296[b] 1309	1340	0.629	0.957	0.301	0.541	0.240	0.717
4	AN	1207[b] 1176	1340	0.679	1.027	0.322	0.610	0.288	0.739
5	TMS	1142	1090	0.734	1.086	0.201	0.603	0.342	0.744
6	PC	1139	1190	0.664	1.074	0.263	0.603	0.340	0.734
7	BT	1220	1020	0.674	1.016	0.297	0.560	0.203	0.753
8	AC	1128	1120	0.677	1.099	0.198	0.550	0.352	0.747
9	TMP	970	580	0.697	1.278	0.096	0.557	0.461	0.817
10	DMF	919[b] 900	670	0.665	1.349	−0.005	0.536	0.541	0.808
11	DMA	900	400	0.713	1.373	−0.048	0.500	0.548	0.825
12	Me_2SO	883	380	0.790	1.409	−0.042	0.577	0.619	0.790

[a-c] As in Table IV.

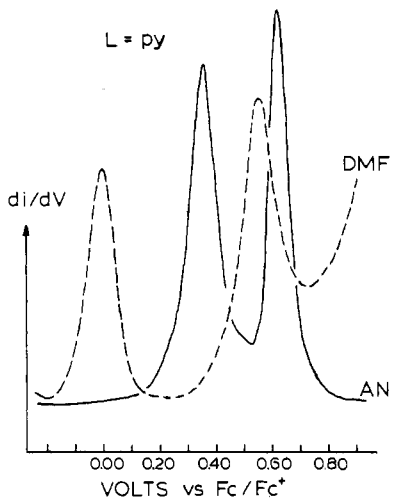

Figure 2. Differential pulse polarograms vs. Fc/Fc$^+$ for the dimer $(bpy)_2Ru^{II}Cl(pyz)Ru^{II}(NH_3)_4py(PF_6)_3$ in acetonitrile (AN) and dimethylformamide (DMF) (0.1 M $(TEA)PF_6$ supporting electrolyte, Pt-disk electrode, 1 mV/s sweep rate, 5-mV pulse amplitude, 0.2-s drop time).

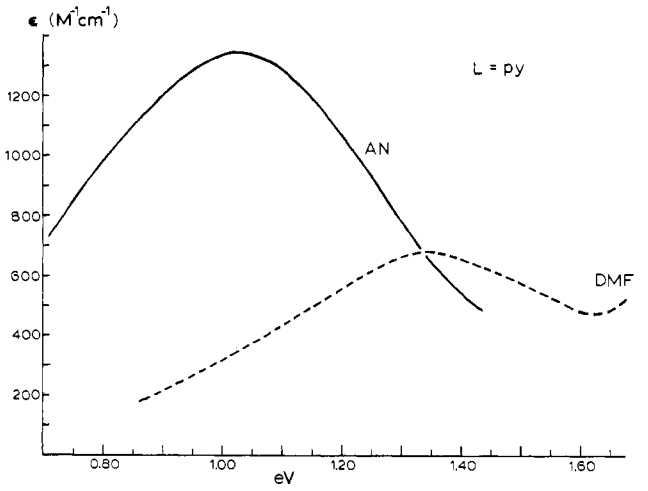

Figure 3. Near-infrared spectra for the $(bpy)_2Ru^{II}Cl(pyz)Ru^{III}(NH_3)_4py^{4+}$ mixed-valence dimer in acetonitrile and DMF.

in Figure 2. Figure 3 shows the near-IR spectra of this dimer in acetonitrile and DMF.

Ion-Pairing Effects. Early in this study we attempted to use Br_2 vapor as our oxidant in the spectrophotometric experiments and encountered seemingly anomalous results in the low donor number solvents. Redetermination with $Fe(bpy)_3^{3+}$ as oxidant revealed that substantial spectral shifts were being induced in the low donor number solvents (DN < ~14) due to ion pairing of the product bromide ion and the $Ru^{III}(NH_3)_4L$ fragment. In nitromethane, for example, it was found that for L = NH_3 $\lambda_{max}(Br_2)$ = 1008 nm while $\lambda_{max}(Fe(bpy)_3^{3+})$ = 1332 nm. In

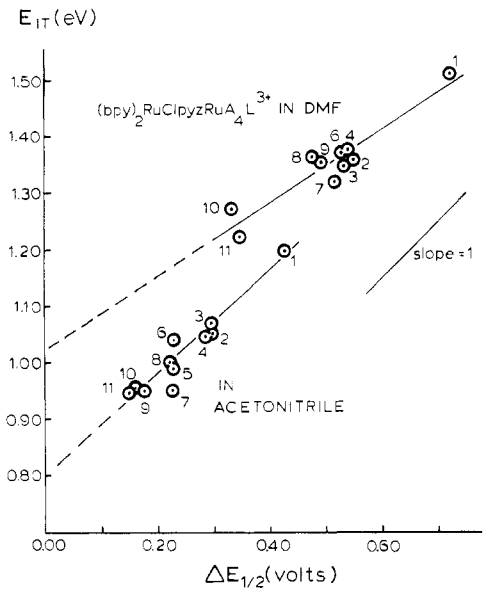

Figure 4. E_{IT} vs. $\Delta E_{1/2}$ (difference in first and second half-wave potentials) as L is varied in acetonitrile and DMF. For a key to the ligands see Tables II and III.

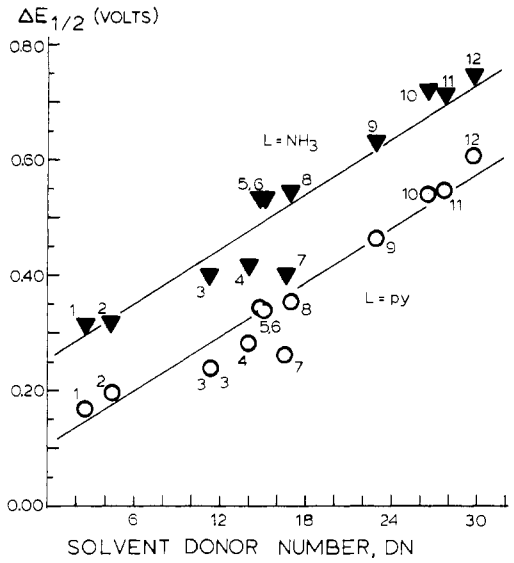

Figure 5. $\Delta E_{1/2}$ vs. solvent donor number for the dimers L = NH_3 (triangles) and L = py (circles). For the solvent key see Table I.

acetonitrile, however, this difference drops to 12 nm, and in DMF it is −2 nm. These last values are within experimental error of each other.

A more subtle medium effect was observed by comparing the spectral results obtained in a pure solvent with those obtained in the 0.1 M TEAH/solvent mixture used in the electrochemical measurements. Inspection of Tables IV and V shows that no systematic and experimentally significant variations are found except for the L = NH_3 dimer in the weak donor solvents NM and NB. In this case the presence of 0.1 M TEAH shifts λ_{max} from 1332 nm in pure nitromethane to 1248 nm and from 1315 nm in pure nitrobenzene to 1210 nm. This correction to E_{IT} has the effect of bringing the points for NM and NB onto the line formed by the other solvents in Figure 6. Curiously, such shifts are *not* observed for the L = py dimer and in fact these two points are both below the line in Figure 6. This would imply either that the trans pyridine ligand on the $Ru^{III}(NH_3)_4$ fragment disrupts ion pairing with PF_6 or that the $\Delta E_{1/2}$ value measured in the L = py case is predominantly due to electrostatic and resonance effects rather than true redox asymmetry. Another possible complication regarding these two points is the onset of valence delocalization (vide infra).

Variations in L. Tables II and III summarize the electrochemical and spectroscopic results obtained when L is varied in both AN and DMF as solvents, respectively. The variations in L are capable of sweeping $\Delta E_{1/2}$ over a 394 mV range in DMF and a range of 271 mV in AN. In all cases it is the redox potential of the first $Ru^{II/III}$ wave that moves as L is varied. The potential of the second wave (the $(bpy)_2RuCl(pyz)$ fragment) moves only very slightly.[24] The smallest $\Delta E_{1/2}$ value of 0.149 V is obtained for L = 1,10-phenanthroline in AN. These peaks are still sufficiently well-resolved that any correction for overlapping would be negligible.[25]

Figure 4 shows the relationship between E_{IT} and $\Delta E_{1/2}$ obtained in both AN and DMF. The slope of the line in AN is 0.98 ± 0.15 eV/V at 95% confidence with a correlation coefficient of 0.895. In DMF the slope is 0.69 ± 0.20 eV/V with a correlation coefficient of 0.88. Due to the grouping of the points, the data in DMF are rather inconclusive other than to indicate that the slope is probably no greater than 1. The line in AN is considerably more informative and supports the 1:1 energetic relationship expected on the basis of Figure 1 and in fact found between these spectroscopic and thermodynamic quantities in similar studies involving both intervalence-transfer[17a,b,28] and metal–ligand charge-transfer[29a] transitions. It is possible, however, that the $\Delta E_{1/2}$ values for L = phen and bpy in AN are anomalously large and cause the slope of the line to be too high.[21] Another possible complicating factor is that the radii a_2 of the Ru^{III} ammine acceptor sites are significantly larger for the L = bpy and L = phen complexes at the early part of the line than for the pentaammine complex at the upper end. This would have the effect of decreasing any DCT-related X_{outer} value by about 35% as calculated in eq 3 and thereby once again increasing the slope of the line.

The 1:1 energetic relation $\delta E_{IT}/\delta(\Delta E_{1/2}) = 1$ is predicated on the assumption that $\delta(\Delta E_{1/2}) = \delta(\Delta E)$ as represented in Figure 1 (vide infra). In the case of variations in L this is probably a fairly reasonable assumption except for possible small variations in the entropic component of $\Delta E_{1/2}$ due to the same radius variations mentioned above. With use of the relationships established by Hupp and Weaver it can be calculated that this effect will amount to less than 40 mV upon going from L = NH_3 to L = bpy ($-NH_3$) in acetonitrile.[12c]

Variations with Solvent. The positions of the redox potentials of the ammine-bearing ends of the two dimers investigated (L = NH_3, py) were found to vary strongly as a function of solvent (see Tables IV and V). This behavior is readily explained as being due to the well-known donor number effect arising from hydrogen bonding between solvent molecules acting as Lewis bases and the acidic protons of the coordinated ammines.[9,12,13,14b] Figure 5 shows the correlations obtained between $\Delta E_{1/2}$ and the solvent donor number. For the pentaammine dimer we find a slope of 0.017 ± 0.002 V/DN and an intercept of 0.24 ± 0.05 V with a correlation coefficient of 0.966. For the tetraammine dimer with L = py we find 0.016 ± 0.002 V/DN and an intercept of 0.09 ± 0.04 V with a correlation coefficient of 0.969.

These slopes are slightly less than what would be expected on the basis of the approximate −0.0047 V/DN per ammine value observed by Weaver and co-workers in a series of ruthenium

(24) These small variations, though treated as being negligible here, form the basis for an analysis of the coupling between the redox sites as presented in ref 23.
(25) Richardson, D. E.; Taube, H. *Inorg. Chem.* **1981**, *20*, 1278.
(26) Calculated as the average of X on Y and Y on X linear least-squares fits by using a standard program.[27]
(27) Mortimer, R. S. *Mathematics for Physical Chemistry*; Macmillan: New York, 1981; p 298.
(28) Goldsby, K. A.; Meyer, T. J. *Inorg. Chem.* **1984**, *23*, 3002.
(29) (a) Juris, A.; Belsir, P.; Barigelletti, F.; Zelewsky, A.; Balzani, V. *Inorg. Chem.* **1986**, *25*, 256. (b) Lever, A. B. P.; Picchens, S. R.; Miner, P. L.; Licoccia, S.; Ramaswamy, B. S.; Magnell, K. *J. Am. Chem. Soc.* **1981**, *103*, 6800. (c) Crutchley, R. J.; Lever, A. B. P. *Inorg. Chem.* **1982**, *21*, 2276. (d) Dodsworth, E. S.; Lever, A. B. P. *Chem. Phys. Lett.* **1984**, *112*, 567. (e) Dodsworth, E. S.; Lever, A. B. P. *Chem. Phys. Lett.* **1985**, *119*, 61.

Scheme I

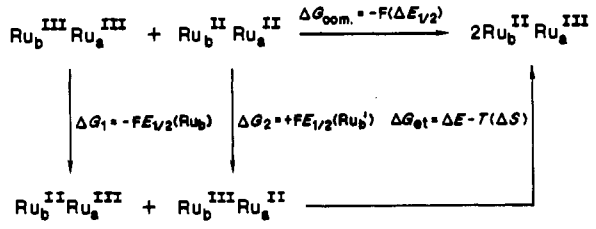

ammine monomers.[12d] The predicted value for the pentaammine dimer would be 0.24 V/DN and that for the tetraammine pyridine dimer would be 0.19 V/DN if the $E_{1/2}(Ru_b)$ potentials were solvent-invariant. Careful inspection of the $E_{1/2}(Ru_a)$ and $E_{1/2}(Ru_b)$ values in Tables IV and V (or of Figure 2), however, shows that the $E_{1/2}(Ru_b)$ potential does in fact track that of the $E_{1/2}(Ru_a)$ potential to a small extent due to the electronic coupling between sites.[24] This phenomenon, along with any possible disruptive interactions between the $(bpy)_2Ru^{II}Cl(pyz)$ moiety and the ruthenium ammine to solvent molecule hydrogen bonding at the other side of the bridge, would explain the rather shallow slopes. In principle one would still expect the tetraammine compound to exhibit a 20% lesser slope than the pentaammine. Apparently the precision of our data is insufficient to reveal this.

Relationship between $\Delta E_{1/2}$ and ΔE. At this point it becomes important to consider in detail the relationship between the electrochemically measured free energy difference $\Delta E_{1/2}$ and the internal energy difference between redox isomers ΔE as shown in Figure 1. ΔE represents an internal energy difference, which in the absence of pressure–volume work is the same as the enthalpy difference for the reaction shown in eq 6. $\Delta E_{1/2}$, on the other

$$(bpy)_2ClRu_b^{II}(pyz)Ru_a^{III}(NH_3)_4L^{4+} \underset{}{\overset{\Delta E}{\rightleftharpoons}} (bpy)_2ClRu_b^{III}(pyz)Ru_b^{II}(NH_3)_4L^{4+} \quad (6)$$

hand, represents the free energy change for the comproportionation reaction shown in eq 7, where we adopt the shorthand notation

$$Ru_b^{II}Ru_a^{II} + Ru_b^{III}Ru_a^{III} \overset{\Delta G_{com}}{\rightleftharpoons} 2Ru_b^{II}Ru_a^{III} \quad (7)$$

Ru_b and Ru_a for the bis(bipyridine)- (second DPP peak) and ammine-bearing (first DPP peak) metals, respectively, and it is readily shown that

$$\Delta G_{com} = -n\mathcal{F}(\Delta E_{1/2}) \quad (8)$$

($\mathcal{F}$ is the Faraday constant and in this case $n = 1$). The relationship between ΔE and $\Delta E_{1/2}$ can be made apparent by considering a thermochemical cycle similar to the one discussed by Goldsby and Meyer[28] (Scheme I). The quantity $E_{1/2}(Ru_b')$ is a fictitious one and would be less than the $E_{1/2}(Ru_b)$ potential both because the electrostatic influence of the Ru_a^{II} center would be different from that of the Ru_a^{III} center which pertains in the measureable $E_{1/2}(Ru_b)$ case and because reduction to form $Ru_b^{II}Ru_a^{II}$ must disrupt any delocalization stabilization in the mixed-valence state whereas reduction to form $Ru_b^{II}Ru_a^{III}$ is favored by the delocalization energy. From Scheme I it is straightforward to show that

$$\Delta E = \Delta E_{1/2} + T(\Delta S) + (E_{1/2}(Ru_b') - E_{1/2}(Ru_b)) \quad (9)$$

where we now express ΔE and $T(\Delta S)$ in eV/mol. Taking derivatives with respect to $\Delta E_{1/2}$ yields

$$\delta(\Delta E)/\delta(\Delta E_{1/2}) = 1 + \frac{\partial}{\partial(\Delta E_{1/2})}(T(\Delta S) + (E_{1/2}(Ru_b') - E_{1/2}(Ru_b))) \quad (10)$$

From work on related monomeric systems, the entropy of intramolecular electron transfer ΔS is expected to depend upon the sizes and charge types of the ions as well as the solvent acceptor number.[12c] No strong dependence upon $\Delta E_{1/2}$ in the absence of changes in these other quantities would be expected. The quantity $E_{1/2}(Ru_b') - E_{1/2}(Ru_b)$ would vary slightly with $\Delta E_{1/2}$ insofar as the delocalization energy between the sites will vary with $\Delta E_{1/2}$, but this effect will be numerically small (vide infra; see also ref 23 and 30). Thus we find agreement with the intuitive expectation that $\delta(\Delta E)/\delta(\Delta E_{1/2}) \cong 1$.

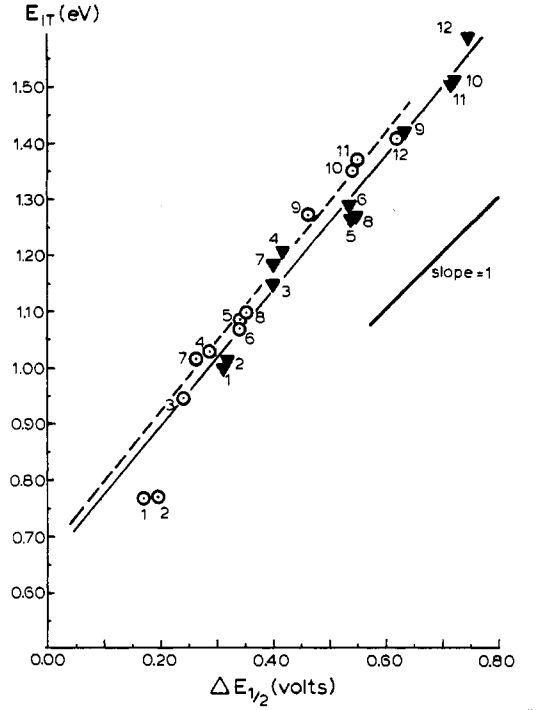

Figure 6. E_{IT} vs. $\Delta E_{1/2}$ as solvent is varied for L = NH_3 (triangles) and L = py (circles). For the solvent key see Table I.

As indicated above, for a given dimer in a series of solvents the $T(\Delta S)$ term, and hence $\Delta E_{1/2}$, should vary with the solvent acceptor number. Dual-parameter fits of the $\Delta E_{1/2}$ data using the solvent donor numbers and acceptor numbers together, however, lead to no significant improvement in the correlation shown in Figure 5. Neither does inclusion of $1/D_s$, as might be expected if solvent dielectric properties were important in defining the electrostatic component of $\Delta E_{1/2}$.[31] From these facts we conclude that the predominant solvent effect on $\Delta E_{1/2}$ is enthalpic in nature and dependent solely upon the solvent donor number within the precision of our data.

There is recent evidence to suggest that in fact it is the free energy of intramolecular electron transfer, ΔG, rather than internal energy, ΔE, which should be considered as the appropriate factor in defining the thermodynamic asymmetry component of E_{IT}.[32,33] As far as the work presented here is concerned, the difference is unimportant since it is solvent-induced variations in the *enthalpic* component of $\Delta E_{1/2}$ that are causing the changes in the thermodynamics of intramolecular electron transfer.

Relationship between $\Delta E_{1/2}$ and E_{IT} As the Solvent Is Varied. Figure 1 shows that for the simplest possible case in which E_{FC} is invariant with ΔE one would observe $\delta E_{IT}/\delta(\Delta E) = 1$ and hence, by virtue of eq 10 and 5 $\delta E_{IT}/\delta(\Delta E_{1/2}) = 1$ as long as E_{FC} is invariant with ΔE. This behavior is indeed observed to be the case as L is varied in acetonitrile. If, however, E_{FC} changes as ΔE is varied, $\delta E_{IT}/\delta(\Delta E_{1/2})$ will deviate from unity. This is observed to be the case in Figure 6, where the relationship between E_{IT} and $\Delta E_{1/2}$ as the solvent is varied for the L = NH_3 and L = pyridine dimers is shown. For the pentaammine dimer we find a slope of 1.23 ± 0.08 eV/V, at 95% confidence with an intercept 0.65 ± 0.07 eV and a correlation coefficient of 0.971. For the tetraammine pyridine dimer we find a slope of 1.26 ± 0.07 eV/V, an intercept of 0.67 ± 0.05 eV, and a correlation coefficient of

(30) Salaymeh, F.; de la Rosa, R.; Curtis, J. C., manuscript in preparation.
(31) Sutton, J. E.; Taube, H. *Inorg. Chem.* **1981**, *20*, 3125.
(32) (a) Marcus, R. A.; Sutin, N. *Comments Inorg. Chem.*, in press. (b) Haim, A. *Ibid.* **1985**, *4*, 113.
(33) Hupp, J. T., private communication.

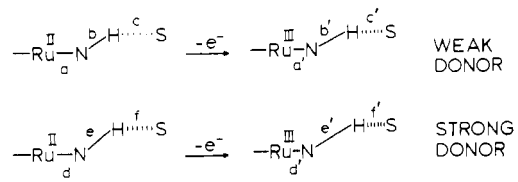

Figure 7. Schematic diagram of the bond length changes that occur about the ruthenium ammine group upon electron transfer in both weak and strong donor solvents.

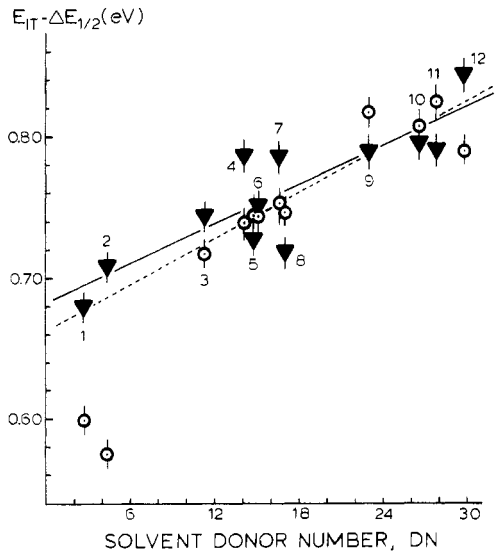

Figure 8. $E_{IT} - \Delta E_{1/2}$ vs. solvent donor number for L = NH_3 (triangles) and L = py (circles). For the solvent key see Table I.

0.986 (omitting the nitromethane and nitrobenzene data for the reasons discussed earlier).

The slopes of the lines in Figure 6 stand in sharp contrast to those obtained in the cases where L is varied. The data indicate that E_{FC} is increasing with $\Delta E_{1/2}$ in such a way as to make the quantity $\delta E_{IT}/\delta(\Delta E_{1/2})$ exceed unity by an experimentally significant amount.

The origin of this effect is readily understood if we consider the nature of the specific solvent–solute interaction taking place at the ammine end of each molecule. In strong donor solvents the Ru(III) ammine fragments are stabilized relative to their Ru(II) forms and hence the $Ru^{II/III}$ redox potential decreases. This comes about because of the more acidic nature of the Ru(III) ammine protons[34] and their subsequently increased H-bond donation ability.[35] There should also be a greater redox-state-dependent change in the nuclear coordinates and force constants of the solvent–solute complex as the solvent donicity goes up and the overall enthalpic consequences of hydrogen bonding become more important.[10,35] This idea is illustrated in Figure 7, where, from the bond length variation rules as set forth by Gutmann and co-workers, we would expect to find the following inequalities to apply to the various bond lengths indicated: $a > d$, $b < e$, $c > f$; $a > a'$, $b < b'$, $c > c'$; $d > d'$, $e < e'$, $f > f'$. If we define, for example, $\delta a = |a - a'|$, then we would predict $\delta a < \delta d$, $\delta b < \delta e$, and $\delta c < \delta f$. This result contradicts the idea of a constant Δq with varying ΔE as shown in Figure 1 and would indicate that any solvent donor number induced variations in ΔE will also bring about variations in Δq.

Solvent Dependence of the Franck–Condon Energy. From eq 9 and the apparent unimportance of the solvent dependence of the $T(\Delta S)$ term we can assert that $\Delta E \cong \Delta E_{1/2}$ + (constant terms) as the solvent is varied. Since E_{FC} as illustrated in Figure 1 is equal to $E_{IT} - \Delta E$, it is clear that E_{FC} should be proportional to the quantity $E_{IT} - \Delta E_{1/2}$. Changes in the Franck–Condon energy with solvent, δE_{FC}, should be equal to $\delta(E_{IT} - \Delta E_{1/2})$.

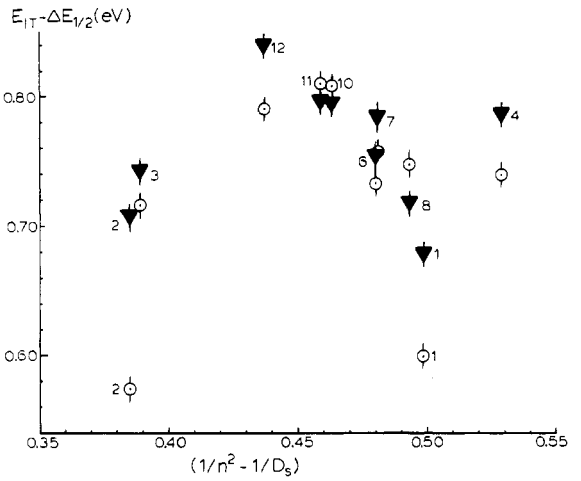

Figure 9. $E_{IT} - \Delta E_{1/2}$ vs. the dielectric continuum solvent term $1/n^2 - 1/D_s$. For the solvent key see Table I.

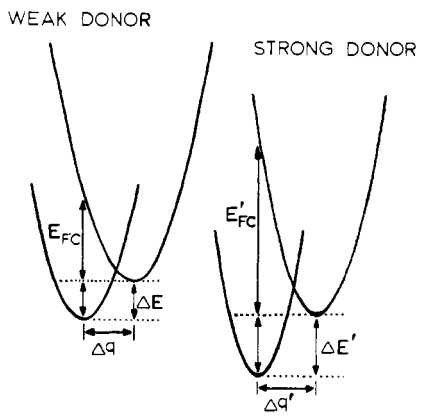

Figure 10. Schematic representation of the potential energy surfaces for the dimers $(bpy)_2Ru^{II}Cl(pyz)Ru^{III}(NH_3)_4L^{4+}$ as solvent donor number is increased.

Figure 8 shows a plot of the quantity $E_{IT} - E_{1/2}$ vs. solvent donor number. Though the data are rather scattered, the correlation is quite clear. For the pentaammine dimer the slope is found to be 0.0055 ± 0.0017 eV/DN with an intercept of 0.68 ± 0.04 eV and a correlation coefficient of 0.743. For the tetraammine pyridine dimer (omitting NB and NM) we find a slope of 0.0060 ± 0.0017 eV/DN, an intercept of 0.66 ± 0.04 eV, and a correlation coefficient of 0.825.

These correlations are not improved by inclusion of the $1/n^2 - 1/D_s$ parameter of dielectric continuum theory (DCT) in a dual-parameter-fitting procedure. In fact the lack of correlation with the DCT parameter is made obvious in Figure 9. The pattern displayed in Figure 8 matches fairly well with that which is obtained when one simply plots donor number vs. $1/n^2 - 1/D_s$.

A further important aspect of the solvent barrier is revealed if we consider the shape of the IT band as $\Delta E_{1/2}$ is varied. Table V shows us that the band becomes very sharp and narrow as judged from ϵ_{max} and $\Delta\nu_{1/2}$ for the $(bpy)_2Ru^{II}Cl(pz)Ru^{III}(NH_3)_4py^{4+}$ dimer in nitromethane and nitrobenzene where the $\Delta E_{1/2}$ values are reduced down to 0.170 and 0.196 V, respectively, via the donor number effect on the potential of the ammine fragment. Such band shape changes are generally taken as being indicative of a change from a localized to a delocalized electronic structure and will be favored by a small redox asymmetry[23] and a small trapping barrier.[1a] *No* such band sharpening is observed in Table II, where variations in the unique ligand in acetonitrile as solvent are used to bring $\Delta E_{1/2}$ down to similarly small values

(34) Navon, G.; Waysbort, D. *J. Chem. Soc., Chem. Commun.* **1971**, 1410.
(35) Work in progress in this laboratory would indicate that the equilibrium constant for preferential solvation of Me_2SO in acetonitrile about a ruthenium(III) ammine complex is approximately 12-fold that of the corresponding ruthenium(II) ammine complex.
(36) Gutmann, V.; Resch, G.; Linert, W. *Coord. Chem. Rev.* **1982**, *43*, 133.
(37) Creutz, C. *Inorg. Chem.* **1978**, *17*, 3723.
(38) Hupp, J. T., private communication.

(0.175 V for L = 2,6-Me_2-pz, 0.149 V for L = phen ($-NH_3$)). These data suggest that the determining factor that allows for the onset of electron delocalization in the former case is the smaller trapping barrier in nitromethane and nitrobenzene (donor numbers of 2.7 and 4.4) relative to acetonitrile (donor number 14.1).

Potential Energy Surfaces. From the foregoing discussion based on the bond length variation rules and the experimental evidence set forth here, we are in a position to arrive at a fairly detailed picture of the effects of solvent on the potential energy surfaces defining optical and thermal electron-transfer processes in systems such as these. Figure 10 shows the qualitative changes that would be expected upon going from a weak to a strong donor solvent. From the diagram it can be seen that $\Delta E' > \Delta E$, $\Delta q' > \Delta q$, and $E_{FC}' > E_{FC}$. We note that *both* redox isomers are stabilized upon going to a higher donor number solvent. It is the greater stabilization of the $Ru^{III}A_4L$-bearing isomer relative to that of the $Ru^{II}A_4L$-bearing isomer that causes $E_{1/2}(Ru_a)$ to fall with increasing solvent donicity. The increase in E_{FC} will be due not only to the increased Δq, as discussed earlier, but also to the increase in force constants defining the H-bonding interaction in the solvation sphere as the solvent donicity is increased.

A more quantitative mapping of solvent effects on these surfaces may become possible in the future given sufficient study of such factors as the thermodynamics of preferential solvation about Ru(II) and Ru(III) ammine moieties[35] and vibrational data precise enough to reveal solvent effects on the NH stretching frequencies.

Inner-Sphere Franck–Condon Barrier. The intercepts in Figure 8 are due to the reorganizational energy that would still remain in a zero donor number solvent, the slight band-shifting effect resulting from overlapping multiple transitions,[7] a subtractive component due to the fact that $\Delta E_{1/2}$ exceeds ΔE by some fairly constant amount arising from electrostatic and resonance effects,[21] and an additive component due to any residual DCT-related solvent barrier that might remain. If we choose a least lower bound of 0.12 V for the electrostatic correction, then the IT band energy in the absence of any donor number dependent Franck–Condon energy and in the absence of any thermodynamic asymmetry, ΔE, becomes $\geq 0.79 \pm 0.06$ eV. An approximate upper bound of 0.31 eV can be calculated for the DCT term by using eq 3 if an average effective value of 0.47 is used for $1/n^2 - 1/D_s$ and the radii are picked as being 6.8 and 4.4 Å.[12c,39] If the hydrogen-bonded layer of solvent molecules around the ammine end of the dimer adds to the effective radius the value of this barrier would be lower. Combining all these considerations leads to a predicted value of 0.5 ± 0.2 eV for for the intercept if we ignore the overlapping, multiple-transition correction.

Plots of the IT band energy vs. the DCT term $1/n^2 - 1/D_s$ for the symmetrical dimers $((bpy)_2RuCl)_2L_b^{3+}$ where the bridging ligand L_b is varied yield intercepts on the order of 0.71 ± 0.04 eV. These intercepts can be related to the inner-sphere Franck–Condon barrier when corrected for the overlapping, multiple-band effect.[7,19] It should be noted, however, that they still exceed what would be expected for X_{inner} on the basis of known structural data.[19] A recent, nine-solvent redetermination of the solvent dependence of E_{IT} for the symmetrical $[(NH_3)_4Ru]_2(4,4'\text{-bpy})^{5+}$ dimer confirms earlier results yielding a good correlation with DCT and gives an intercept of 0.54 ± 0.04 eV if the data in D_2O and methanol are ignored. Averaging these would predict an intercept of 0.63 ± 0.06 eV for an asymmetric system such as $(bpy)_2RuCl(pyz)Ru(NH_3)_5^{4+}$. The value for the tetraammine pyridine species might be slightly higher but would not be expected to differ greatly.[37,39] It is noteworthy that the observed intercepts derived here for asymmetric systems from donor number plots and the predicted intercepts derived from the entirely different DCT form of solvent dependence in symmetric dimers are in reasonable agreement.

Concluding Remarks

One interesting contrast presented by this work is that the solvent dependence in these systems is completely dictated by specific, noncontinuum effects whereas that for the $[(NH_3)_5Ru]_2(4,4'\text{-bpy})^{5+}$ dimer is found to be of the DCT type (vide supra).[37,38] This is quite surprising until one considers that lengthening the bridging ligand from pyrazine to 4,4'-bpy and substituting a ruthenium pentaammine moiety for the larger $(bpy)_2RuCl$ group will increase the magnitude of the DCT solvent dependence by a factor of about 2.7 as predicted from eq 3 and known structural data.[1a] Even this, however, does not dispel the quandary completely since the presence of twice as many ruthenium–ammine groups should also double the importance of the solvent donicity effect on the Franck–Condon barrier.

That redox-state-dependent hydrogen bonding to solvent in mixed-valence dimers containing ruthenium–ammine groups should introduce a substantial Franck–Condon barrier to optical electron transfer is not surprising, and in fact the existence of hydrogen-bonding-dependent Franck–Condon energies has also been recognized as being important for organic chromophores.[40] It is striking, however, that the DCT solvent effect is so completely supplanted by the noncontinuum solvent effect for the molecules investigated here. One would expect that an appropriately designed mixed-valence system should be identifiable which would respond simultaneously to *both* kinds of solvent-induced barriers. Work along these lines is currently under way.[41]

The elucidation of the noncontinuum solvent effect as revealed in this work is made possible because of the high degree of complementarity that exists between thermodynamic and spectroscopic data on mixed-valence systems in general. The strong theoretical and experimental relationship between optical and thermal electron transfer is highlighted if we note the parallelism between this work and the growing body of work demonstrating the importance of noncontinuum solvent effects on thermal electron transfers in related mononuclear systems.[12-15]

Separation of the reorganizational barrier to electron transfer into well-defined inner- and outer-sphere components is clearly inappropriate when strong, specific solvent–solute interactions are operative. The continuing refinement of our microscopic understanding of ionic solvation and its consequences regarding electron transfer promises to allow for a more and more detailed mapping of the potential energy surfaces (and hence reaction-coordinate diagrams) for these relatively large and complicated molecular systems.

Acknowledgment. Thanks are gratefully expressed to the Research Corp. for the support making this work possible. We also wish to acknowledge helpful discussions with Dr. Joe Hupp of Northwestern University.

(39) Brown, G. M.; Sutin, N. *J. Am. Chem. Soc.* **1979**, *101*, 883.

(40) (a) Pimentel, G. C. *J. Am. Chem. Soc.* **1957**, *79*, 3323. (b) Martin, M. M. *Chem. Phys. Lett.* **1975**, *35*, 105. (c) Del Bene, J. E. *J. Am. Chem. Soc.* **1978**, *100*, 1395. (d) Taylor, P. R. *J. Am. Chem. Soc.* **1982**, *104*, 5248. (e) Johnson, G. E.; Limburg, W. W. *J. Phys. Chem.* **1984**, *88*, 2211.

(41) Fung, E. Y.; Curtis, J. C., work in progress.